PRODUCTION OF $K\bar{K}$-PAIRS IN PHOTON–PHOTON COLLISIONS AND THE EXCITATION OF THE TENSOR MESON f′(1515)

TASSO Collaboration

M. ALTHOFF, R. BRANDELIK [1], W. BRAUNSCHWEIG, K. GATHER, F.J. KIRSCHFINK, K. LÜBELSMEYER, H.-U. MARTYN, G. PEISE, J. RIMKUS, H.G. SANDER, D. SCHMITZ, H. SIEBKE, D. TRINES, W. WALLRAFF
I. Physikalisches Institut der RWTH Aachen, Germany [11]

H. BOERNER [2], H.M. FISCHER, H. HARTMANN, E. HILGER, W. HILLEN, G. KNOP, L. KÖPKE, H. KOLANOSKI, H. KÜCK, R. WEDEMEYER, N. WERMES [3], M. WOLLSTADT
Physikalisches Institut der Universität Bonn, Germany [11]

H. BURKHARDT, S. COOPER, J. FRANZKE, D. HOCHMAN [4], H. HULTSCHIG, P. JOOS, W. KOCH, U. KÖTZ, H. KOWALSKI [5], A. LADAGE, B. LÖHR, D. LÜKE, P. MÄTTIG, K.H. MESS, D. NOTZ, J. PYRLIK, D.R. QUARRIE [6], R. RIETHMÜLLER, W. SCHÜTTE, P. SÖDING, G. WOLF, G. YEKUTIELI [4]
Deutsches Elektronen-Synchrotron, DESY, Hamburg, Germany

R. FOHRMANN, H.L. KRASEMANN, P. LEU, E. LOHRMANN, D. PANDOULAS, G. POELZ, P. SCHMÜSER, B.H. WIIK
II. Institut für Experimentalphysik der Universität Hamburg, Germany [11]

I. AL-AGIL, R. BEUSELINCK, D.M. BINNIE, A.J. CAMPBELL, P.J. DORNAN, B. FOSTER, D.A. GARBUTT, T.D. JONES, W.G. JONES, J. McCARDLE, J.K. SEDGEBEER
Department of Physics, Imperial College London, England [12]

K.W. BELL [7], M.G. BOWLER, I.C. BROCK [8], R.J. CASHMORE, R. CARNEGIE [9], P.E.L. CLARKE, R. DEVENISH, P. GROSSMANN, J. ILLINGWORTH, S.L. LLOYD, G.L. SALMON, J. THOMAS, T.R. WYATT, C. YOUNGMAN
Department of Nuclear Physics, Oxford University, England [12]

J.C. HART, J. HARVEY, J. PROUDFOOT, D.H. SAXON, P.L. WOODWORTH
Rutherford Appleton Laboratory, Chilton, England [12]

D. HEYLAND, M. HOLDER
Gesamthochschule Siegen, Germany

E. DUCHOVNI, Y. EISENBERG, U. KARSHON, G. MIKENBERG, D. REVEL, E. RONAT, A. SHAPIRA
Weizmann Institute, Rehovot, Israel [13]

and

T. BARKLOW, M. CHERNEY, T. MEYER [10], G. RUDOLPH, H. VENKATARAMANIA, E. WICKLUND, SAU LAN WU, G. ZOBERNIG
Department of Physics, University of Wisconsin, Madison, WI, USA [14]

Received 11 November 1982

(for footnotes see next page)

0 031-9163/83/0000–0000/$ 03.00

We have observed exclusive production of K^+K^- and $K_s^0K_s^0$ pairs and the excitation of the f′(1515) tensor meson in photon–photon collisions. Assuming the f′ to be produced in a helicity 2 state, we determine $\Gamma(f' \to \gamma\gamma)\, B(f' \to K\bar{K}) = 0.11 \pm 0.02 \pm 0.04$ keV. The non-strange quark content of the f′ is found to be less than 3% (95% CL). For the θ(1640) we derive an upper limit for the product $\Gamma(\theta \to \gamma\gamma)\, B(\theta \to K\bar{K}) < 0.3$ keV (95% CL).

We present the first measurement of the two-photon excitation of the f′(1515) meson in the reaction:

$$e^+e^- \to e^+e^- + \gamma\gamma \to e^+e^- + f' .$$

The f′ was detected via:

$$f' \to K^+K^- , \tag{1}$$

and

$$f' \to K_s^0K_s^0 \to \pi^+\pi^-\pi^+\pi^- . \tag{2}$$

Detection of the scattered e^+ or e^- was not required.

Within the framework of SU(3) a measurement of $\Gamma(f' \to \gamma\gamma)$ and the knowledge of $\Gamma(f^0 \to \gamma\gamma)$ allow the determination of a deviation of the $J^{PC} = 2^{++}$ nonet from ideal mixing.

The experiment was performed with the TASSO detector at the DESY storage ring PETRA. A description of the detector can be found elsewhere [1]. The present data sample corresponds for channel (1) to an integrated luminosity of 74 pb^{-1} at beam energies between 7 and 17.5 GeV and for channel (2) to 79 pb^{-1} at beam energies between 14 and 18.3 GeV, with most of the data around 17 GeV. The data reported here were taken with the following triggers:

(1) Four or more charged tracks, or (2) any two charged tracks having associated signals in inner time-of-flight counters separated by more than 154° in azimuth, or (3) two or more charged tracks originating from the interaction region.

These triggers were based on the central proportional and drift chamber processors, which required the track momenta perpendicular to the beam, p_T, to exceed preselected nominal values, leading to momentum dependent track detection efficiencies. For the first part of the data, only triggers (1) and (2) were used; the track finding efficiency was 50% at $p_T = 0.20$ GeV/c, increasing to about 95% for $p_T \geqslant 0.37$ GeV/c. The majority of the data (~65 pb^{-1}) was taken with the additional trigger (3), which was the most efficient one for our present study. For this trigger, a lower preselected nominal p_T value was used, leading to a track detection efficiency of 50% at $p_T = 0.17$ GeV/c and of 95% for $p_T \geqslant 0.29$ GeV/c. This trigger required the event vertex to be within 15 cm of the interaction point along the beam direction. The vertex was found by using the cathode information of the central proportional chamber [2].

We first discuss the analysis of the K^+K^- final state. Candidates for two-photon produced events with two charged particles were selected requiring two oppositely charged tracks with $p_T > 0.20$ GeV/c and $|\cos\vartheta| \leqslant 0.8$, where ϑ is the polar angle with respect to the beam axis. In order to reject lepton pairs from one photon annihilation and cosmic rays the sum of the measured charged particle momenta had to be less than 40% of the beam momentum, and the two tracks had to be non-collinear by more than 5 degrees. To minimize uncertainties introduced by energy loss, decays, secondary interactions and multiple Coulomb scattering, the momentum of each track had to be larger than 0.35 GeV/c.

For the identification of K^+K^- pairs we used time-of-flight (TOF) measurements from the 48 scintillation counters surrounding the cylindrical drift chamber at

[1] Present address: IST, Darmstadt, Germany.
[2] Present address: KEK, Oho-Machi, Japan.
[3] Present address: SLAC, Stanford, CA, USA.
[4] Minerva Fellow, on leave from Weizmann Institute, Rehovot, Israel.
[5] On leave at CERN, Geneva, Switzerland.
[6] Present address: Fermilab, Batavia, IL, USA.
[7] On leave from Rutherford Appleton Laboratory, Chilton, England.
[8] Present address: Carnegie–Mellon University, Pittsburgh, USA.
[9] On leave from Carleton University, Ottawa, Canada.
[10] Present address: Texas A + M University, TX, USA.
[11] Supported by the Deutsches Bundesministerium für Forschung und Technologie.
[12] Supported by the UK Science and Engineering Research Council.
[13] Supported by the Minerva Gesellschaft für Forschung mbH.
[14] Supported by the US Department of Energy contract AC02-76ER00881.

a radius of 1.32 m. The rms time resolution is 445 ps for particles passing through the centre of the counters, improving approximately linearly to 265 ps for particles passing through close to the end of the scintillators. The efficiency for the TOF measurement was 92%, averaged over the full period of data taking.

Since the TOF separation of kaons from the lighter particles deteriorates with increasing particle momentum, only events with both tracks having momenta lower than 0.9 GeV/c were taken for the analysis. For each particle in this data sample we calculated the square of the mass from the measured track length, momentum and time-of-flight (m^2_{TOF}). In fig. 1 we plot m^2_{TOF} of the negative particle versus m^2_{TOF} of the positive one, restricting the vector sum of the transverse momenta of the final state particles $|\Sigma p_{\mathrm{T}}|$ to be less than 0.1 GeV/c. While most of the events – electron, muon and pion pairs – cluster around zero, about 0.8% of the entries are $\mathrm{K}^+\mathrm{K}^-$ pairs. In this analysis we do not distinguish between electrons, muons and pions and will refer to them all as "pions".

Candidates for kaon pairs were preselected by applying a cut $m^2_{\mathrm{TOF}} > 0.1\ \mathrm{GeV}^2$ for both tracks (compare fig. 1). To select kaon pairs, three gaussian weights (n = "π", K, p)

$$W(\mathrm{n}) = \exp[-(t_{\mathrm{m}} - t_{\mathrm{n}})^2/2\sigma^2] \tag{3}$$

were assigned to each particle, corresponding to the three hypotheses that the particle is a "pion", kaon or proton. Here t_{m} is the measured TOF, t_{n} is the expected TOF for hypothesis n, and σ is the rms time resolution (265–445 ps) as discussed above. The weight $W(\mathrm{K})$ for each track had to be consistent within 3 sd with the kaon hypothesis.

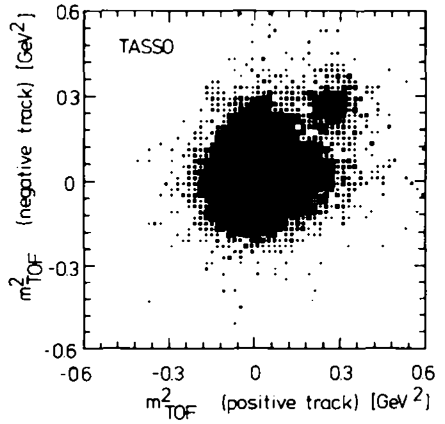

Fig. 1. Scatter plot of m^2_{TOF} of the negative particle versus m^2_{TOF} of the positive one for two-photon events with two charged particles after a cut of $|\Sigma p_{\mathrm{T}}| < 0.1$ GeV/c was applied.

To separate kaon pairs from "π""π", "π"K, "π"p or $\mathrm{p\bar{p}}$ pairs the following cuts were applied to the event weights, i.e. to the product of the particle weights:

$$\begin{aligned}
&W(\mathrm{K}^+)\,W(\mathrm{K}^-) > 10 \cdot 125\quad W(\pi^+)\,W(\pi^-)\,,\\
&W(\mathrm{K}^+)\,W(\mathrm{K}^-) > 10 \cdot 0.2\quad W(\mathrm{K}^\pm)\,W(\pi^\mp)\,,\\
&W(\mathrm{K}^+)\,W(\mathrm{K}^-) > 10 \cdot 0.2\quad W(\mathrm{p})\,W(\bar{\mathrm{p}})\,,\\
&W(\mathrm{K}^+)\,W(\mathrm{K}^-) > 10 \cdot 1\quad\ \ W(\mathrm{p})\,W(\pi^-)\,.
\end{aligned} \tag{4}$$

The factors (125, 0.2, 0.2, 1) in (4) take roughly into account the observed relative abundances of the different particle pair combinations. The extra factor of 10 ensures that even in the worst case the probability to be $\mathrm{K}^+\mathrm{K}^-$ for a pair selected in (4) is larger than 90%.

For $\gamma\gamma$ final states, the net transverse momentum is predominantly small, which allows a rejection of events with undetected particles. After a cut of $|\Sigma p_{\mathrm{T}}| < 0.1$ GeV/c, the remaining background of $\mathrm{K}^+\mathrm{K}^-$ events with additional undetected particles was estimated to be 2%.

The $\mathrm{K}^+\mathrm{K}^-$ mass distribution of the 419 events surviving these cuts is shown in fig. 2a. A clear enhancement in the region of the f′ is seen. The contribution from misidentified particle pairs to this f′ signal was estimated from the tails of the measured m^2_{TOF} distributions and found to be less than 5%.

In order to understand the shape of this mass distribution we simulated the reaction $\mathrm{e}^+\mathrm{e}^- \to \mathrm{e}^+\mathrm{e}^- + \gamma\gamma \to \mathrm{e}^+\mathrm{e}^- + \mathrm{K}^+\mathrm{K}^-$ in the detector by a Monte Carlo program. Events were generated according to

$$\frac{\mathrm{d}\sigma_{\mathrm{e^+e^-\to e^+e^-K\bar{K}}}}{\mathrm{d}W_{\gamma\gamma}\,\mathrm{d}\omega\,\mathrm{d}\cos\theta^*} = \frac{\mathrm{d}\mathcal{L}(W_{\gamma\gamma},\omega)}{\mathrm{d}W_{\gamma\gamma}\mathrm{d}\omega}\,\frac{\mathrm{d}\sigma_{\gamma\gamma\to\mathrm{K\bar{K}}}(W_{\gamma\gamma},\cos\theta^*)}{\mathrm{d}\cos\theta^*}\,, \tag{5}$$

where the symbol ω represents the variables of the two γ's other than the centre of mass energy $W_{\gamma\gamma}$, θ^* is the angle between the photon and kaon direction in the $\gamma\gamma$ centre of mass system and $\mathcal{L}$ is the two-photon luminosity function for transverse photons [3]. These events were passed through the same cuts as described above for the real events.

Fig. 2d shows the percentage of accepted events of

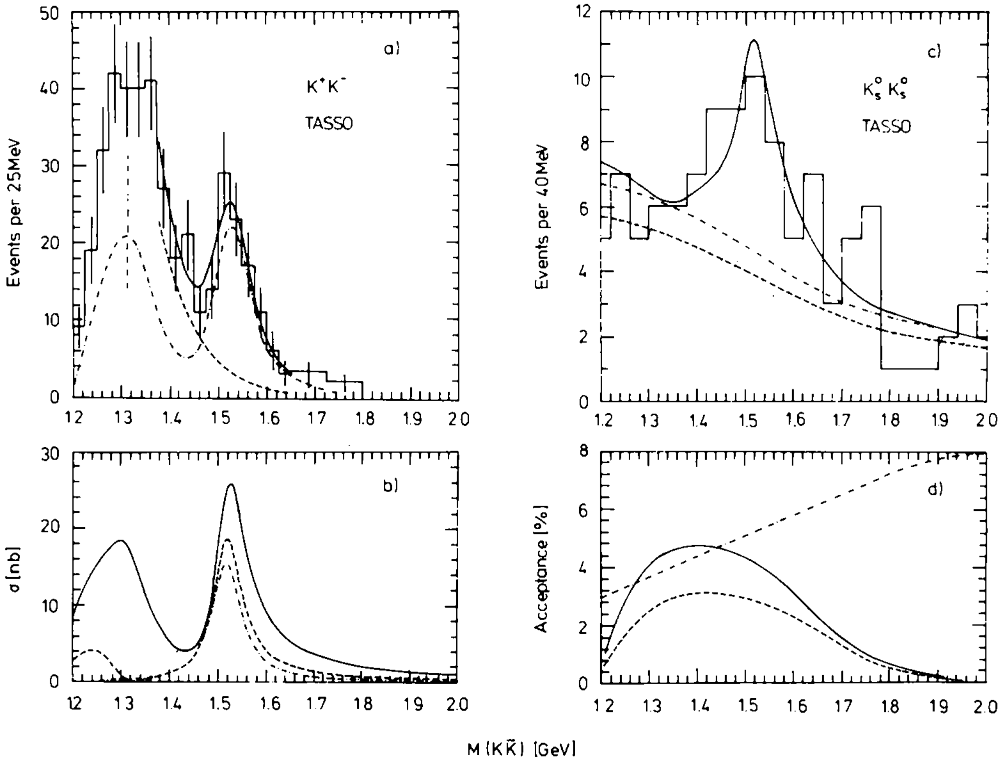

Fig. 2. (a) $M(K^+K^-)$ distribution. The full curve is the result of a fit as described in the text. The dashed–dotted curve is the contribution from the interfering f^0, A_2 and f′ resonances. The background contribution is given by the dashed line. The error on the dashed–dotted curve reflects the uncertainty in the $\gamma\gamma$ partial widths and $K\bar{K}$ branching ratios of f^0 and A_2. (b) Calculated cross sections for $\gamma\gamma \to K\bar{K}$ (no acceptance effects are included). The solid curve refers to the K^+K^- final state (constructive interference between A_2, f^0 and f′). The dashed curve refers to the $K^0\bar{K}^0$ final state (destructive interference between the A_2 and the f^0 and f′). The dashed–dotted curve is the f′ contribution assuming no interference. See text for details. (c) $M(K_s^0K_s^0)$ distribution for events with fitted $|\Sigma p_T| < 0.15$ GeV/c. The full curve is the result of a fit to a sum of the interfering f^0, A_2 and f′ resonances and a background (dashed–dotted line) as described in the text. The dashed curve is the estimate of the absolute background not due to $K_s^0K_s^0$ production, with an uncertainty given by the shaded area. (d) The acceptance as function of the $K\bar{K}$ effective mass. The dashed curve is for a K^+K^- isotropic decay angular distribution; the solid curve is for a K^+K^- helicity $\lambda = 2$ distribution; the dashed–dotted curve is for a $K_s^0K_s^0$ $\lambda = 2$ distribution.

the type $\gamma\gamma \to K^+K^-$ generated with a flat distribution in $\cos\theta^*$ (dashed curve) as well as with a $\sin^4\theta^*$ distribution (solid curve). The latter distribution applies for the decay of $J^{PC} = 2^{++}$ mesons in the $\gamma\gamma$ helicity $\lambda = 2$ state, which is expected to dominate the $\gamma\gamma$ production of the tensor mesons f^0, A_2, f′ [4].

Comparing the $M(K^+K^-)$ mass distribution in fig. 2a with the acceptance curves in fig. 2d one finds that the drop-off in the data below 1.3 GeV is caused by the acceptance. Around 1.5 GeV the acceptance varies smoothly and cannot explain the structure in the f′ region.

The contribution of the 2^{++} nonet resonances to the $\gamma\gamma \to K\bar{K}$ cross section can be expressed as a coherent sum of the f^0, A_2 and f′ amplitudes [5]:

$$\sigma_{\gamma\gamma\to K\bar{K}}(W_{\gamma\gamma}) = (40\pi/W_{\gamma\gamma}^2)$$
$$\times |[\Gamma(f^0 \to \gamma\gamma)B(f^0 \to K\bar{K})]^{1/2}\,\mathrm{BW}(f^0)$$
$$\pm [\Gamma(A_2 \to \gamma\gamma)B(A_2 \to K\bar{K})]^{1/2}\,\mathrm{BW}(A_2)$$
$$+ [\Gamma(f' \to \gamma\gamma)B(f' \to K\bar{K})]^{1/2}\,\mathrm{BW}(f')|^2 \,. \tag{6}$$

$\mathrm{BW(R)} = M\sqrt{\Gamma}/(M^2 - W_{\gamma\gamma}^2 - iM\Gamma)$ is a relativistic Breit–Wigner amplitude, where M is the mass and Γ is the energy dependent width of the resonance R. A barrier penetration factor was used as in ref. [6] [‡1].

For footnote see next page.

$B(R \to K\bar{K})$ is the $K\bar{K}$ branching ratio of the resonance R, and $\Gamma(R \to \gamma\gamma)$ its $\gamma\gamma$ partial width. According to SU(3) predictions [5], the plus sign of the second term applies to the K^+K^- final state; the minus sign applies to $K^0\bar{K}^0$, where the interference between the isovector (A_2) and the isoscalars (f^0, f') is destructive.

In fig. 2b the calculated cross sections (6) are shown for the final states K^+K^- (solid curve) and $K^0\bar{K}^0$ (dashed curve). The values for the mass, total width and $B(R \to K\bar{K})$ of the resonances and $\Gamma(f^0 \to \gamma\gamma) = 2.95 \pm 0.40$ keV were taken from ref. [7]. We used the value $\Gamma(A_2 \to \gamma\gamma) = 0.66 \pm 0.11^{+0.29}_{-0.16}$ keV [8] and assumed $\Gamma(f' \to \gamma\gamma)\,B(f' \to K\bar{K}) = 0.11$ keV. It is clear from fig. 2b that for the K^+K^- final state the interference near the f' region yields a mass spectrum which is very different from the spectrum in which no interference is assumed (dashed- dotted curve).

To determine the $\gamma\gamma$ coupling of the f' we fitted the K^+K^- mass spectrum (fig. 2a) between 1.375 and 1.650 GeV with a maximum likelihood method using Poisson statistics. The fits included the contributions from the interfering f^0, A_2, f' resonances as given in eq. (6). $\Gamma(f' \to \gamma\gamma)\,B(f' \to K\bar{K})$ was treated as a free parameter in the fit. For all contributions acceptance effects were included assuming a helicity $\lambda = 2$ angular distribution.

In addition to the resonances, non-resonant K^+K^- production has to be taken into account. A simple Born approximation [9] gives too large a cross section in the fit region. This Born term has to be modified due to strong interaction effects which are expected to suppress the cross section at higher values of $M(K^+K^-)$. In the absence of a rigorous description of the mass dependence of this non-resonant K^+K^- production, several background parametrizations were tried, such as a gaussian shape or a shape $[M(K^+K^-) - M_0]^{-n}$ with $1 \leqslant n \leqslant 6$ and M_0 a free parameter. They all gave a reasonable description of the data.

The result of one of these fits is shown in fig. 2a (full curve). The background parametrization used (dashed curve) is the one which yielded the central value for $\Gamma(f' \to \gamma\gamma)\,B(f' \to K\bar{K})$. The contribution from the resonances is given by the dashed-dotted curve. The following value was obtained for the product of the $K\bar{K}$ branching ratio and $\gamma\gamma$ width of the f':

$$\Gamma(f' \to \gamma\gamma)\,B(f' \to K\bar{K})$$
$$= 0.11 \pm 0.02\,(\text{stat.}) \pm 0.04\,(\text{syst.})\ \text{keV}\,.$$

The systematic uncertainty comes from various contributions:
- different background parametrizations as described above (± 0.025 keV),
- errors in $\Gamma(f^0 \to \gamma\gamma)$, $\Gamma(A_2 \to \gamma\gamma)$, $B(f^0 \to K\bar{K})$, $B(A_2 \to K\bar{K})$ (± 0.015 keV),
- uncertainty in the acceptance and overall normalization (± 0.020 keV).

We now describe the analysis of the $K^0_SK^0_S$ final state. Candidates for the two-photon excitation of the f' meson, with a subsequent decay into two K^0_S's each of which decays into $\pi^+\pi^-$ were selected from the sample of events with two positive and two negative tracks. All tracks were required to have a $p_T > 0.1$ GeV/c and $|\cos\vartheta| < 0.87$. The sum of the measured charged particle momenta had to be less than 8 GeV/c.

In order to suppress events with additional undetected particles, we demanded $|\Sigma\, p_T| < 0.15$ GeV/c, yielding a sample of 6370 events. In fig. 3a we show the effective mass distribution $M(\pi^+\pi^-)$ where all particles were assumed to be pions (four combinations per event). Most of these data are due to $\rho^0\rho^0$ production [10], however a clear indication of K^0_S production is seen. The evidence for double K^0_S production can be seen from the $M(\pi^+\pi^-)$ distribution of events where the other $\pi^+\pi^-$ combination was required to be in the K^0_S mass region of 0.475–0.525 GeV (shaded histogram in fig. 3a – note change of scale). The fraction of K^0_S in the shaded histogram is enhanced. In figs. 3b–d we show the mass recoiling against a K^0_S in three regions of $W_{\gamma\gamma}$. Clear evidence for $K^0_SK^0_S$ is seen in the $W_{\gamma\gamma}$ interval between 1.35 and 1.65 GeV.

The $\pi^+\pi^-\pi^+\pi^-$ events were fitted to the $K^0_SK^0_S$ hypothesis (2 constraint fit). 156 events with a fitted $|\Sigma\, p_T| < 0.15$ GeV/c yielded an acceptable chi-square probability $[P(\chi^2) > 0.1\%]$. The $M(K^0_SK^0_S)$ distribution for these events is shown in fig. 2c, where a clear signal at the $f'(1515)$ is seen.

The reaction $e^+e^- \to e^+e^- + \gamma\gamma \to e^+e^- + K^0_SK^0_S \to e^+e^- + \pi^+\pi^-\pi^+\pi^-$ was simulated by a Monte Carlo program. $K^0_SK^0_S \to 4\pi$ events originating from f^0, A_2,

[‡1] The parameter r, as defined in ref. [6], was set for all three resonances to 1 fm. The cross section at the f' peak is lowered by 8% when r is increased to 2 fm.

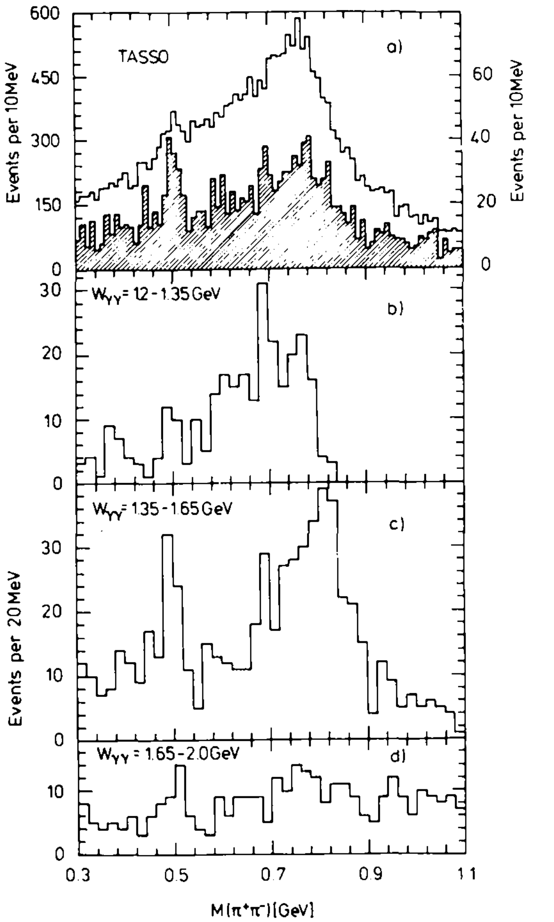

Fig. 3. $M(\pi^+\pi^-)$ distributions for $\gamma\gamma \to \pi^+\pi^-\pi^+\pi^-$ events with $|\Sigma p_T| < 0.15$ GeV/c. (a) $M(\pi^+\pi^-)$ distribution (4 entries per event). Also shown (shaded) is the $M(\pi^+\pi^-)$ recoiling against the K_s^0 mass (0.475–0.525 GeV). The ordinate scale on the left (right) corresponds to the full (shaded) histogram. (b)–(d) The recoiling mass against the K_s^0 as defined above for three different $W_{\gamma\gamma}$ bins.

f′ with a $\lambda = 2$ angular distribution were generated according to eqs. (5) and (6). Since the dominant background in our sample at small $|\Sigma p_T|$ is $\rho^0\rho^0$ production, we generated $\rho^0\rho^0$ and four pion phase-space events according to our measured cross sections [10]. All Monte Carlo events were analysed with the same cuts and kinematical fit as the real data.

The background not due to $K_s^0K_s^0$ production was estimated from the data as follows: Events having one $M(\pi^+\pi^-)$ combination below and the other one above the K_s^0 mass (side bands), were passed through the same kinematical fit, constraining the two $M(\pi^+\pi^-)$ combinations to values of 0.4 and 0.6 GeV, respectively and requiring $P(\chi^2) > 0.1\%$. Since the variation of this background as function of $M(\pi^+\pi^-)$ is expected to be small around 0.5 GeV (see fig. 3), the $M(4\pi)$ distribution of the fitted events from the side bands as defined above is a good estimate of the absolute background (dashed curve in fig. 2c). The shaded area in fig. 2c represents the uncertainty in this background determination. The reliability of this method was verified by repeating the same procedure with $\rho^0\rho^0$ and four pion phase-space Monte Carlo events. The amount of $K_s^0K_s^0$ events in fig. 2c above the absolute background in all $M(4\pi)$ regions is consistent with the $K_s^0K_s^0$ rates before the kinematical fit (figs. 3b–d).

The f^0, A_2, f′ distribution of events generated according to eq. (6) (with the minus sign for the second term) and the background discussed above were fitted to the data of fig. 2c in the mass region 1.2–1.9 GeV. The full curve in fig. 2c shows the result of this fit, where $\Gamma(f' \to \gamma\gamma)\,B(f' \to K\bar{K})$ was taken as a free parameter and the background normalization was allowed to vary (dashed–dotted curve).

Correcting for unobserved decay modes and assuming $\lambda = 2$, we obtain $\Gamma(f' \to \gamma\gamma)\,B(f' \to K\bar{K}) = 0.11 \pm 0.03$ (stat.) $\pm$ 0.04 (syst.) keV. In this fit we used the PDG [7] values for the f′ mass and width. The systematic error takes into account the uncertainties in the background estimates, the kinematical fit parameters and the overall normalization.

The decay angular distribution of events in the invariant mass range between 1.45 and 1.65 GeV was studied in both K^+K^- and $K_s^0K_s^0$ final states. The data are consistent with both the $\lambda = 2$ and the $\lambda = 0$ assumptions, while an isotropic distribution in $\cos\theta^*$ can be ruled out. If a $\lambda = 0$ helicity is assumed for the f′, the partial width obtained from the K^+K^- ($K_s^0K_s^0$) channel will be larger by about a factor of three (two) compared to the $\lambda = 2$ result, due to the change of the acceptance and a different interference pattern. The average result from $f' \to K^+K^-$ and $f' \to K_s^0K_s^0$ (assuming $\lambda = 2$) is:

$$\Gamma(f' \to \gamma\gamma)\,B(f' \to K\bar{K}) = 0.11 \pm 0.02\,(\text{stat.}) \pm 0.04\,(\text{syst.})\ \text{keV}\,. \qquad (7)$$

This result is consistent with the upper limit of $\Gamma(f' \to \gamma\gamma)\,B(f' \to K^+K^-) < 0.6$ keV (95% CL) given in ref. [11].

Using the world average for $\Gamma(f^0 \to \gamma\gamma)$ [7], we compare the product (7) with SU(3) predictions. The mixing angle of the 2^{++} nonet, Θ_M, is known to be close to the ideal mixing value of 35.3° [7,12]. A calculation of $\Gamma(f' \to \gamma\gamma)$, using the mixing angle given by the Gell-Mann–Okubo (GMO) quadratic mass formula (28° ± 3°) [7], yields $\Gamma(f' \to \gamma\gamma) = 0.11^{+0.10}_{-0.065}$ keV, where phase-space corrections were included. Since $K\bar{K}$ is the dominant decay mode of the f′ [7], this result is consistent within errors with our result (7) for a wide range of $B(f' \to K\bar{K})$ values. Assuming $B(f' \to K\bar{K}) \geqslant 0.5$ [12], our measurement (7) yields the following limits on the SU(3) mixing angle [‡2]:

$$25.4° < \Theta_M < 34.7° \quad (95\% \text{ CL}) .$$

The lower limit on Θ_M constrains the non-strange quark content in the f′ to be less than 3% (95% CL) independent of $B(f' \to K\bar{K})$. This constraint also holds in the model of ref. [13] which allows for gluonic admixtures to the resonances. Our $\Gamma(f' \to \gamma\gamma)$ result is however inconsistent with an extension of this model [14] which predicts a strong suppression of $\Gamma(f' \to \gamma\gamma) < 0.01$ keV.

Recently, a resonant state $\theta(1640)$ decaying into $\eta\eta$ was found in J/ψ radiative transitions [15]. Preliminary results [16] show that there is also a substantial θ branching ratio into $K\bar{K}$. The partial width $\Gamma(\theta \to \gamma\gamma)$ may be larger than $\Gamma(f' \to \gamma\gamma)$ [13,14]. Assuming $J^{PC} = 2^{++}$, $\lambda = 2$ and no interference with the other 2^{++}-states, we derive an upper limit for the product $\Gamma(\theta \to \gamma\gamma)B(\theta \to K\bar{K}) < 0.3$ keV (95% CL).

To summarize, we have observed the excitation of the f′(1515) resonance in photon-photon collisions in both K^+K^- and $K^0_sK^0_s$ decay modes. Assuming $\lambda = 2$ and production according to eq. (6) we determine $\Gamma(f' \to \gamma\gamma)B(f' \to K\bar{K}) = 0.11 \pm 0.02 \pm 0.04$ keV. Using the measured $\gamma\gamma$ width of the f^0, we find that within SU(3) our result is consistent with $\Gamma(f' \to \gamma\gamma)$ as calculated from the mixing angle of the GMO mass formula for any reasonable value of $B(f' \to K\bar{K})$. The non-strange quark content in the f′ is found to be less than 3% (95% CL). With $B(f' \to K\bar{K}) \geqslant 0.5$ we determine the SU(3) mixing angle to be $25.4° < \Theta_M < 34.7°$ (95% CL). An upper limit for the coupling of the $\theta(1640)$ to $\gamma\gamma$ and $K\bar{K}$ yields $\Gamma(\theta \to \gamma\gamma)B(\theta \to K\bar{K}) < 0.3$ keV (95% CL).

[‡2] Our result also allows a second solution $4.3° < \Theta_M < 13.2°$ (95% CL); however such a large deviation from ideal mixing is inconsistent with the measured small value of $B(f' \to \pi\pi)$ [12].

We gratefully acknowledge the support by the DESY directorate and the tremendous efforts of the PETRA machine group, in particular Dr. K. Steffen and Dr. D. Degèle, for successfully increasing the luminosity with the new minibeta insertions. We wish to thank the technical service groups at DESY and all the engineers and technicians at the collaborating institutions for their invaluable help. We are grateful to Dr. H.J. Lipkin, Dr. H.R. Rubinstein, Dr. B. Schrempp and Dr. F. Schrempp for useful discussions. One of us (Y.E.) wishes to thank the Minna–James–Heineman Stiftung of Hannover for partial support. Those of us from outside DESY wish to thank the DESY directorate for the hospitality extended to us while working at DESY.

[1] TASSO Collab., R. Brandelik et al., Phys. Lett. 83B (1979) 261; Z. Phys. C4 (1980) 87.
[2] S. Jaroslawski, Nucl. Instrum. Methods 176 (1980) 263.
[3] J. Field, Nucl. Phys. B168 (1980) 477; B176 (1980) 545 (E).
[4] B. Schrempp et al., Phys. Lett. 36B (1971) 463.
[5] H.J. Lipkin, Nucl. Phys. B7 (1968) 321; Proc. EPS Intern. Conf. on High energy physics (Palermo, 1975) p. 609;
D. Faiman et al., Phys. Lett. 59B (1975) 269.
[6] TASSO Collab., R. Brandelik et al., Z. Phys. C10 (1981) 117.
[7] Particle Data Group, Phys. Lett. 111B (1982) 1.
[8] C. Edwards et al., Phys. Lett. 110B (1982) 82;
CELLO Collab., H.-J. Behrend et al., Phys. Lett. 114B (1982) 378.
[9] H. Terazawa, Rev. Mod. Phys. 45 (1973) 615.
[10] TASSO Collab., R. Brandelik et al., Phys. Lett. 97B (1980) 448;
TASSO Collab., M. Althoff et al., DESY 82-062 (1982), submitted to Z. Phys. C.
[11] P. Jenni et al., SLAC-PUB-2758 (June 1981), submitted to Phys. Rev. D.
[12] N. Samios, M. Goldberg and B.T. Meadows, Rev. Mod. Phys. 46 (1974) 49;
L. Montanet, The positive parity mesons, CERN/EP 82-69, submitted to Rep. Prog. Phys. (June 1982).
[13] J.L. Rosner, Quark content of neutral mesons, University of Minnesota report (July 1982), submitted to Phys. Rev. D.
[14] J.L. Rosner and S.F. Tuan, Tests of a mixing model for neutral 2⁺ mesons, UH-511-477-82 preprint (1982).
[15] C. Edwards et al., Phys. Rev. Lett. 48 (1982) 458.
[16] E. Bloom, XXIth Intern. Conf. on High energy physics (Paris, 1982), to be published.